ELSEVIER

Computerized Medical Imaging and Graphics 30 (2006) 153–161

Computerized Medical Imaging and Graphics

www.elsevier.com/locate/compmedimag

# Regional analysis of the left ventricle of the heart

François Bernis [a,1], Christophe Léger [a,*], Véronique Eder [b,2]

[a] *Laboratoire d'Électronique, Signaux, Images (LESI), Université d'Orléans, École Polytechnique de l'Université d'Orléans, 12 rue de Blois-BP 6744, 45067 Orléans Cedex 2, France*

[b] *Service de Médecine Nucléaire in vivo et Ultrasons, Centre Hospitalier Universitaire de Tours, Hôpital Trousseau, 37044 Tours Cedex, France*

Received 15 June 2005; received in revised form 27 February 2006; accepted 16 March 2006

**Abstract**

This paper presents a method to analyze the local wall motion of the left ventricle of the heart. Data are sets of points (obtained from various medical imaging modalities) corresponding to surfaces of the left ventricle, which evolve as a function of time. After re-sampling, the surfaces are segmented in order to create regions of equivalent volume. Then, the local cardiac parameters are estimated: evolution of the regional volumes as a function of time, ejection fraction, end-diastolic and end-systolic volumes, end-diastolic and end-systolic instants. The method has been validated using deformable surfaces synthesized from an ellipsoidal model. It has also been tested in vivo on a set of 59 patients using a specially developed software product, which satisfies severe constraints of robustness, real-time, interactivity and ergonomics. The results obtained are similar to those provided by a reference nuclear medicine examination, but the proposed method is faster and gives a more precise localization of the cardiac wall motion anomalies.


*Keywords:* Regional analysis; Fourier interpolation; Surface re-sampling; Left ventricle of the heart; Isotope imaging

## 1. Introduction

Cardiovascular diseases are the main cause of mortality in industrialized countries. It has therefore become a major issue of public health to prevent, to detect, and to monitor their evolution or treatment over time. To establish a diagnosis, cardiologists use various techniques of medical imaging [1] to analyze the cardiac function. Most of the examinations carried out are based on the observation of the left ventricle (LV), and provide global descriptors: volumes (including end-diastolic and end-systolic volumes), mass, and ejection fraction of the LV. Using two-dimensional (2D) images—echocardiography [2] (ultrasound imaging), angiocardiography [3] (X-ray imaging), planar gamma-angiography [4] (isotope imaging)—estimations of such parameters are fast, but based on very rough modeling of the LV [5–7]. The three-dimensional (3D) reconstruction of the LV—myocardial or cavitary gated tomography [8] (isotope imaging), computed tomography [9–10] (magnetic resonance imaging), 3D echocardiography [11] (ultrasound images)— improves model accuracy, and therefore refines estimations [1]. While the indicator, which characterize the global LV function are widely accepted, this is not the case for methods providing local indicators of LV contractility, many of which are controversial [12–14]. However, the accurate localization and quantification of the LV wall motion anomalies are of high interest, since they can reveal ischemic cardiomyopathies [15] and induce therapeutic options [16].

There have been a great number of contributions for the analysis of the LV wall motion [17–20]. Many methods and algorithms of high scientific interest have been proposed, but few of them are currently in use in clinical conditions, due to long computation time, parameter initialization, etc. The work presented in this paper consists of developing a clinically oriented method to analyze local LV wall motion, within regions corresponding to perfusion areas, during a cardiac cycle. The method was validated through two types of experiments. First, an ellipsoidal model was used to generate surfaces that simulate local and temporal cardiac

* Corresponding author. Tel.: +33 238 49 45 63; fax: +33 238 41 73 77.
*E-mail addresses:* christophe.leger@univ-orleans.fr (C. Léger), eder@med.univ-tours.fr (V. Eder).
[1] Tel.: +33 238 49 45 63; fax: +33 238 41 72 45.
[2] Tel.: +33 247 47 59 77; fax: +33 247 47 59 13.

0895-6111/$ - see front matter © 2006 Elsevier Ltd. All rights reserved.
doi:10.1016/j.compmedimag.2006.03.005

dyskinesia, and check the relevance of results. A study was then conducted on a set of real LV surfaces, obtained from SPECT gated blood pool examinations. Particular care was given during implementation of the protocol to satisfy the requirements of physicians: (1) constraint of robustness: algorithms should give correct results with images of standard quality; (2) constraint of real-time processing: the regional analysis should be accomplished within a period below the time needed for a medical consultation; (3) constraint of interactivity: physicians performing the exam should be able to intervene to validate or modulate the results; (4) constraint of ergonomics: the displayed results should be directly interpretable in medical terms. A software product taking into account all these constraints is currently in use at the hospital Trousseau in Tours, France, in the isotopic imaging department.

The paper is organized as follows. First, the complete process that performs the regional analysis of the LV is detailed. Then, experiments carried out to validate the method are presented, and the results obtained are discussed. Finally, future developments are proposed.

## 2. Method

The method developed to segment the LV in regions of interest starts from sets of points corresponding to LV surfaces obtained at different instants of the cardiac cycle. The only specific constraint imposed on the initial samples concerns the existence of an inner origin from which line segments between the inner origin and the initial samples intersect with the surface only once (star-shaped objects). Then, the method is well suited for any convex and various concave organs. For the data presented in this paper, sets of points are the samples of the LV contours extracted within three-dimensional images obtained from cavitary tomographic examinations, but could be obtained from other medical imaging modalities. After positioning manually a three-dimensional mask in one image of the cardiac cycle to isolate roughly the LV cavity, LV contours are determined straightforwardly in each plane of the three-dimensional images by subtracting the thresholded two-dimensional images and their erosion to get contours of one pixel width.

The segmentation method is composed of two parts. As the number of initial samples is not always sufficient (incomplete surfaces reconstructed from several contours), nor uniformly ordered (sets of points without explicit organization), the initial surfaces are first over-sampled, and their samples rearranged. The new surfaces obtained are then segmented using an iterative procedure, in order to create regions of equivalent volume (to be compared easily), and the regional analysis is carried out.

### 2.1. Volume re-sampling

Re-sampling the initial surface provides a double benefit. Not only data are processed as input of the segmentation algorithm, but they are also homogenized when stemming from different imaging modalities without similar properties. The method relies on a basic and fast interpolation technique to satisfy the real-time constraint claimed as a requirement. It uses the Fourier transform [21], in an algorithm called 3DHM for 3D Harmonic Modeling.

#### 2.1.1. Initialization

In a 3D system of coordinates, the LV surface at a given instant is described in spherical coordinates by a function of two variables $\rho(\theta,\varphi)$, $-\pi/2 \leq \theta \leq \pi/2$, $0 \leq \varphi < 2\pi$, relative to an inner origin, which can be chosen as the center of mass of the samples. The $N$ initial samples $\{\rho_i(\theta_i,\varphi_i)\}$, $i \in 0,\ldots,N-1$ of the surface are inserted in a rectangular grid $d(m,n)$, the sides of which represent the $\theta$ and $\varphi$ variables. The dimensions $N_\theta \times N_\varphi$ of the grid give the sampling intervals of the grid in $\theta$ and $\varphi$ directions, $\Delta\theta = 2\pi/N_\theta$ and $\Delta\varphi = 2\pi/N_\varphi$, and the number of samples of the re-sampled surface. Each initial sample $\{\rho_i(\theta_i,\varphi_i)\}$ of the LV surface is inserted in the grid, filled to be doubly periodic in $\theta$ and $\varphi$, as shown in Fig. 1.

When the initial samples are aggregated, or not uniformly distributed (or when the dimensions $N_\theta \times N_\varphi$ of the grid are small), more than one sample $\{\rho_i(\theta_i,\varphi_i)\}$ may correspond to the same position in the grid. In this case, the mean of the samples is assigned to the position. In the same manner, in order to reduce artifacts in $\theta = \pm\pi/2$, the mean of the available samples of the $\theta$ values is assigned to all the corresponding $\varphi$ values, since the vertical radii launched from the center of mass of the LV surface are equal, whatever the $\varphi$ values are.

In most cases, the number and the distribution of the initial samples of the LV surface lead to incomplete grids (Fig. 2a). Each missing value is thus set to zero in $d(m,n)$, and its position saved (in a second grid of the same dimension, in which elements are set to 1 or 0 depending on the presence or absence of the sample in the initial grid). Then, the iterative 3D harmonic modeling by discrete Fourier transform fills up the incomplete grid by carrying out a circular 2D Shannon pseudo-interpolation between initial data.

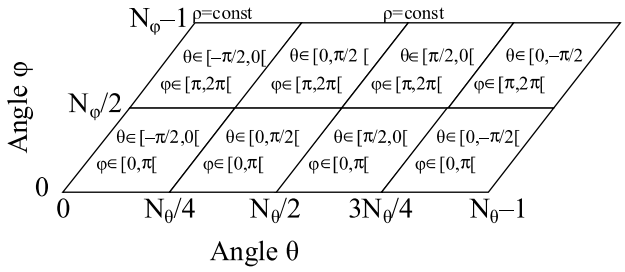


Fig. 1. Structure of the grid doubly periodic in $\theta$ and $\varphi$.

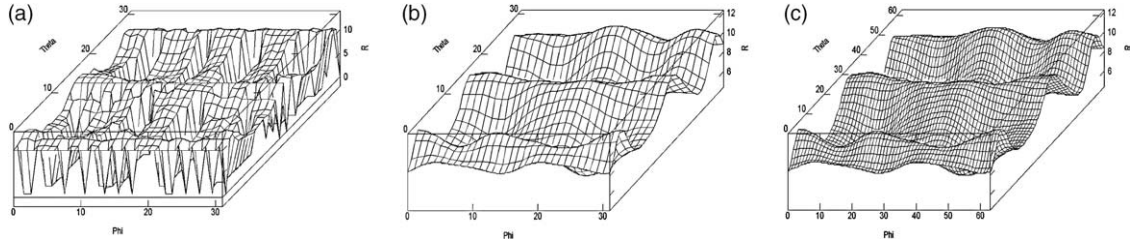


Fig. 2. Surface of the left ventricle in the plane ($\varphi$,$\theta$), with missing samples (a), after interpolation using the 3DHM algorithm (b), after zero-padding (c).

*2.1.2. Interpolation*

Missing data in the incomplete grid $d(m,n)$ are interpolated using an iterative algorithm based on the Fourier transform. At the first iteration, the 2D Fourier transform $D(u,v)$ of the grid (doubly periodic in $\theta$ and $\varphi$) is computed

$$D(u,v) = \Im[d(m,n)] \tag{1}$$

As missing data in the grid contribute mainly to high frequencies in the Fourier domain, a low-pass filtering is applied to reduce discontinuities in the temporal domain (Fig. 3). The transfer function of the low-pass filter is given by the relation:

$$H(u,v) = \begin{cases} 1, & \text{if } |u| < U_0 \text{ and } |v| < V_0, \\ 0, & \text{if not.} \end{cases} \tag{2}$$

An estimation of missing data is then obtained applying the inverse Fourier transform:

$$\hat{d}^0(m,n) = \Im^{-1}[H(u,v)\cdot D(u,v)] \tag{3}$$

To avoid the smoothing of initial data between two iterations, known data from the initial grid $d(m,n)$ are retained. Thus, only the missing samples of the initial grid $d(m,n)$ are modified. The new surface so generated is then used as input for the next iteration, and the process is repeated. The algorithm stops when the estimated values do not vary significantly from one iteration to the following, relative to a fixed threshold $\xi$:

$$\frac{1}{N_\theta \cdot N_\varphi} \sum_{m=0}^{N_\theta - 1} \sum_{n=0}^{N_\varphi - 1} [\hat{d}^j(m,n) - \hat{d}^{j-1}(m,n)]^2 \leq \xi \tag{4}$$

In order to obtain final smooth surfaces, the ultimate interpolated values are not replaced by the known values of the initial grid after the last iteration (Fig. 2b). With the same objective, the number of samples of the interpolated surface is generally increased by zero-padding (Fig. 2c), in order to obtain more samples for rendering or further processing.

The interpolation algorithm is used to distribute initial information over the entire grid, leading to a uniformly sampled surface that interpolates initial data, from a set of non-uniform and incomplete samples. It is very easy to use, as the only adjustable parameters are the dimensions of the low-pass filter used in the Fourier domain, and the error $\xi$ admitted on the initial samples. This iterative algorithm is nevertheless rapid and robust, since computing time can be drastically reduced using a fast Fourier transform algorithm, provided that values $N_\theta$ and $N_\varphi$ are power of two values ($N_\theta = 2^L$ and $N_\varphi = 2^M$ with $L,M \in \Re^2$). Even if the convergence of this algorithm has not been proved yet, one can observe that an error on data less than $\xi = 1\%$ is usually obtained in less than a hundred iterations for LV surfaces.

Once the LV surface has been re-sampled, it needs to be segmented in order to create equivalent regional volumes.

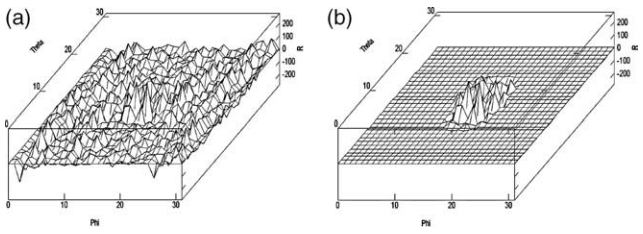


Fig. 3. Real part of the discrete Fourier transform of the grid $d(m,n)$, before (a) and after (b) low-pass filtering.

*2.2. Segmentation in regions of equivalent volume*

At this step, the LV surfaces to be segmented are assumed to be uniformly sampled according to polar angles $\theta$ and $\varphi$ (Fig. 4b), whatever the order of initial samples provided by the acquisition is (Fig. 4a). The regional analysis of the LV is based on a segmentation in regions of medical interest, which corresponds to the 13 myocardial regions of perfusion, as indicated in Fig. 5. The first region, the apex, defines a single region, the volume of which represents 1/13th of the total LV volume. The remaining volume is then separated in three slices corresponding to 4/13th of the total LV volume. Each of the three slices is

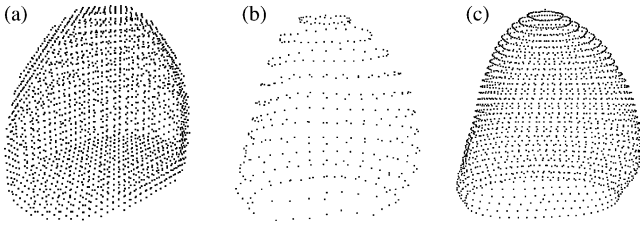


Fig. 4. Samples of the LV surface. Initial samples (a), re-sampled using the 3DHM interpolation algorithm (b), then reordered in planes of constant altitudes (c).

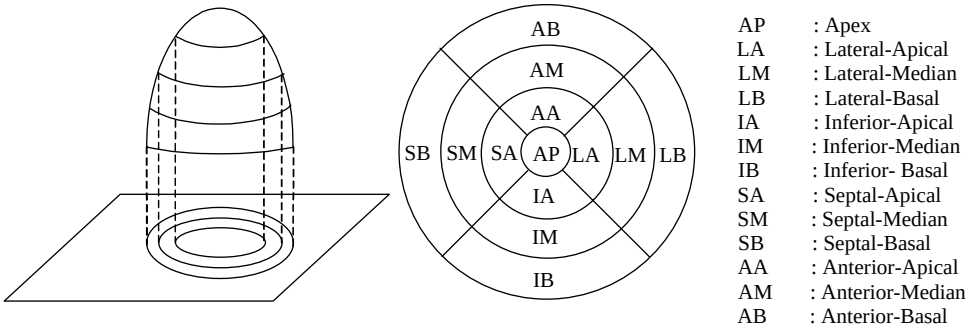


Fig. 5. Left ventricular regions of interest.

geometrically divided into four parts. Thus, the volume of the created regions is about 1/13th of the LV total volume.

The method to segment the LV volumes comprises two steps. First, the samples of the LV surface are aggregated at constant altitudes. Then, the segmentation of regions with equivalent volume is carried out using a specific algorithm called 'volume growing'.

*2.2.1. Sample reordering within planes at constant altitudes*

To reorder the samples of surfaces within planes located at constant altitudes, the LV is divided into $P=N_\theta/2+1$ horizontal slices $2\delta_P$ thick, centered at altitudes $Y_p$, $p\in 0,\ldots,P-1$. All the samples with altitudes between $Y_p-\delta_P$ and $Y_p+\delta_P$ are arbitrarily set to altitude $Y_p$ (Fig. 6). Thus, we obtain $M$ samples of altitude $Y_p$, assumed to be constant to within $\pm\delta_P$, distributed in the interval $[0,2\pi]$. To reduce the errors introduced by this approximation, the number of samples present in the interval $[Y_p-\delta_P, Y_p+\delta_P]$ is increased by zero-padding after the 3DHM interpolation. When several samples are available at the position $\varphi_i=2\pi i/N_\varphi$, $i\in 0,\ldots,N_\varphi-1$, they are averaged. Thus, the LV surface is composed of $N_\varphi$ samples uniformly distributed along $\varphi$ angles, at $P$ altitudes $Y_p$ (Fig. 4c). To ensure data homogeneity at every altitude, $N_\varphi$ equal samples are set for the first and last planes, respectively, at altitudes $Y_0$ and $Y_{P-1}$.

*2.2.2. Region segmentation*

The segmentation algorithm of the LV closed surface is based on an iterative approximation of the ideal cutting height that gives slices of given volume: elementary volumes are estimated and added until the expected volume is reached. The $N_E$ elementary volumes of volume $V_{Ej}$ are calculated from five samples of the surface: two successive samples $(P_{j,p}, P_{j+1,p})$ at a given altitude $Y_p$, the two samples $(P_{j,p+1}, P_{j+1,p+1})$ that correspond to the same position at the closest altitude $Y_{p+1}$, and the center of mass $O$ of the surface (Fig. 7). The estimation of the elementary volumes is given by the relation

$$V_{Ej} = \frac{1}{6}[(\overrightarrow{OP_{j,p}} \times \overrightarrow{OP_{j+1,p}})\cdot\overrightarrow{OP_{j+1,p+1}})] + \frac{1}{6}\cdot[(\overrightarrow{OP_{j+1,p+1}} \times \overrightarrow{OP_{j,p+1}})\cdot\overrightarrow{OP_{j,p}}] \quad (5)$$

where $a\times b$ represents the vector product of vector $a$ and $b$, and $a\cdot b$ the scalar product of vector $a$ and $b$.

By moving gradually from the apex to the base, elementary volumes $V_{Ej}$ at each altitude are summed. The first altitude $Y'_0$ corresponding to a sum of elementary volumes greater or equal to 1/13th of the total volume $V_T$ defines the region $R_0$ of the apex. Similarly, the summation of elementary volumes delineates three volumes greater or equal to $(1+4k)$/13th of the total volume $V_T$, at altitudes $Y'_k$, $1\le k<4$. With altitude $Y'_0$, the latter divide the volume into three slices, which correspond, respectively, to the apical, median and basal LV regions. Each of these slices is then geometrically divided into four sectors, to define the anterior, lateral, inferior and septal LV regions. Finally, samples available within each of the 13 regions are used to estimate volumes $V_{Ri}$, $i\in 0,\ldots,12$, of each region. Although the $V_{Ri}$ volumes represent approximately 1/13th of the total volume $V_T$, they generally differ slightly with real data, since the observed ventricles are not solid of revolution (particularly in the case of pathologic hearts). The total

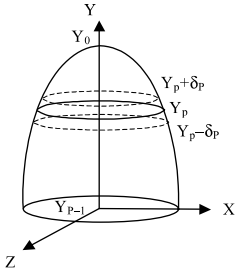


Fig. 6. Division of the LV surface in planes of constant altitudes.

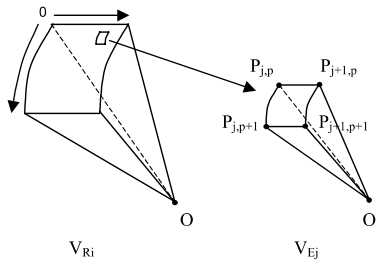


Fig. 7. Regional $V_{Ri}$ and elementary $V_{Ej}$ volumes.

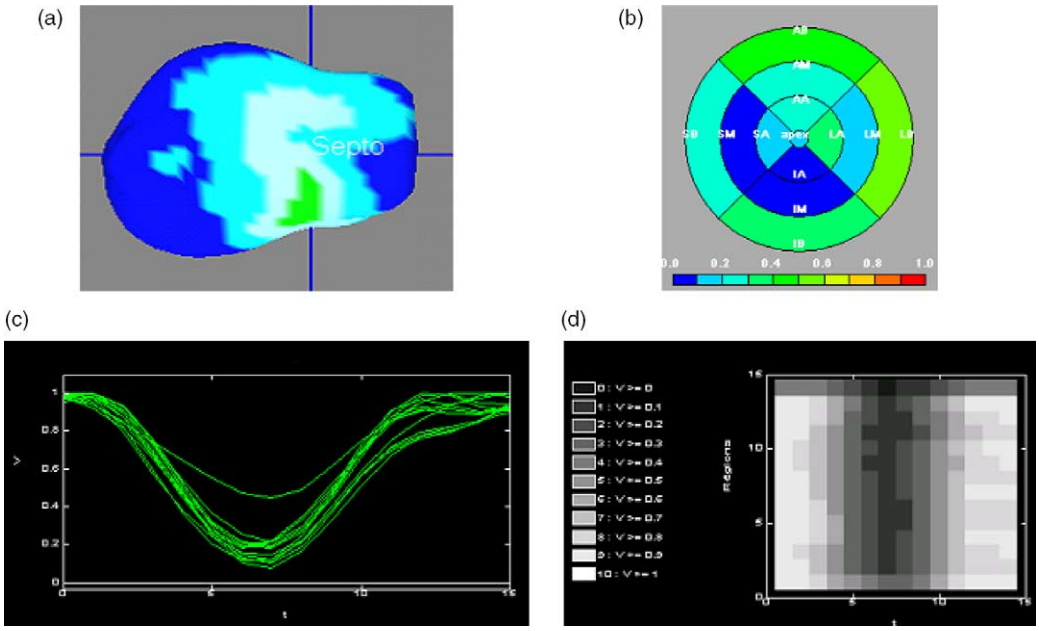


Fig. 8. Evolution of the regional cardiac indicators as a function of time: ejection fraction values mapped on the volumes (a) or projected on bulls-eyes (b), regional volume curves (c) or coded with gray levels (d).

volume $V_T$ of the closed surface of the LV is estimated by summing either the 13 regional volumes $V_{Ri}$ or the $N_E$ elementary volumes $V_{Ej}$:

$$V_T = \sum_{i=0}^{12} V_{Ri} = \sum_{j=0}^{N_E} V_{Ej}, \quad \text{with } N_E = \left(\frac{N_\theta}{2} - 1\right) \cdot N_\varphi. \quad (6)$$

For a regional but dynamic study of the LV, regions of perfusion are determined on the first volume available within the cardiac cycle, and the same spatial positions of the regions are retained for all the other volumes of the cycle.

## 3. Results and discussion

The LV regional analysis observes the regions of perfusion during a cardiac cycle. It qualifies and quantifies the wall motion of regional volumes as a function of time. Five relevant parameters are used to describe the LV wall motion:

- end-diastolic volume $V_D$: the maximum LV volume within the cardiac cycle.
- end-systolic volume $V_S$: the minimum LV volume within the cardiac cycle.
- ejection fraction EF: the normalized difference between extreme volumes within the cardiac cycle:

$$EF = \frac{V_D - V_S}{V_D}. \quad (7)$$

The ejection fraction provides information about the quality of the LV wall motion. A value comprised between 0.5 and 0.7 indicates a healthy heart, whereas a value less than 0.5 or greater than 0.7 denotes a risk of pathology. The estimation of the regional ejection fractions is of great interest to localize precisely on the myocardium potential anomalies of wall motion that could reveal ischemic cardiomyopathies.

- End-diastolic instant $T_D$: instant of the cardiac cycle where the LV volume is maximum.
- End-systolic instant $T_S$: instant of the cardiac cycle where the LV volume is minimum.

All these parameters, usually determined globally, are computed here within regional volumes, then compared with those obtained considering the whole ventricle. The evolution as a function of time of the regional parameters is coded by a color at each instant of the cardiac cycle, then displayed by mapping the colors on dynamic LV volumes (Fig. 8a) or projecting them on bulls-eyes (Fig. 8b). The evolution of the regional volumes is represented quantitatively by plotting the curves of all regions in a single graph (Fig. 8c) or coding evolution information with gray levels (Fig. 8d). By coding the amplitude of the wall motion with a color intensity that ranges between black (no wall motion) and white (maximum wall motion), this representation is useful to identify immediately anomalies of wall motion in each region. In such a representation, a row that is different from the other in the image denotes a singularity of variation amplitude within the corresponding region. Conversely, a vertical reading of the image indicates temporal anomalies of the wall motion (advance or delay of the segmental wall motion compared to the global deformation of the ventricle). The palette of representations available in the

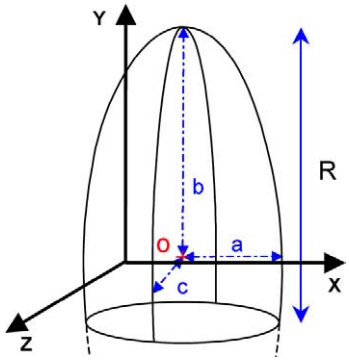


Fig. 9. Parameters of the truncated ellipsoid used to model the LV.

Fig. 10. Example of locally controlled deformable surface obtained with the synthesized ellipsoid.

clinical software developed provides results easily interpretable by physicians of various medical specialties (cardiology, nuclear medicine, ultrasound imaging, etc.)

To validate the method, two studies were carried out. The first one consisted in synthesizing surfaces from an ellipsoidal model. The motion of the ellipsoid walls was controlled within every region of interest of the LV. The generated surfaces were used to check the correspondence between the model deformations and the measured ones. The second study was carried out in vivo on a set of patients presenting cardiac wall motion anomalies.

### 3.1. Validation with a deformable ellipsoidal

As a first approximation, the LV is usually modeled by a truncated ellipsoid given by the equation

$$\left(\frac{x-x_0}{a}\right)^2+\left(\frac{y-y_0}{b}\right)^2+\left(\frac{z-z_0}{c}\right)^2 = 1 \text{ with } y \geq y_0+\frac{2b}{100}R-b \quad (8)$$

where $x_0$, $y_0$, $z_0$ are the coordinates of the center of the ellipsoid not truncated, $a$, $b$, and $c$ represent the three half axes of the ellipsoid, and $R$ is the percentage of truncation of the ellipsoid (see Fig. 9).

A friendly interface was developed to control the evolution of 13 regions of interest, by setting locally the ejection fraction $EF_R$, the diastolic $T_{DR}$ and systolic $T_{SR}$, and simulating regional anomalies of wall motion (Fig. 10). Besides the validation of our segmentation algorithm, this tool can be used for educational purposes to synthesize, visualize and analyze the ventricular dysfunctions.

Table 1 presents the ejection fraction values for 13 regions of interest measured on a synthetic ellipsoid. Noise immunity is checked by adding a white Gaussian noise (mean $\mu=0$, standard deviation $\sigma$, proportional to the radii of the polar development of the synthesized volume samples). The first row of Table 1 displays the values of ejection fractions used to initialize the ellipsoidal model. The next rows show results obtained with 10 and 20% of additive noise. The segmentation algorithm is insensitive to noise, since the average error of the estimated ejection fractions remains much less than 1% when the distance between the volume samples and their center of mass varies more than 20% on average. Fig. 11 shows a bulls-eye representation of the ejection fractions measured regionally.

### 3.2. In vivo study

The second validation tested the method on a set of 59 patients presenting anomalies of the left ventricular wall motion (dilated cardiomyopathies and ischemic cardiomyopathies). The validation of the method is achieved in the following manner. First, a planar gamma-angiography reference examination is carried out under several incidences, to estimate the global ejection fraction of the LV and locate the anomalies of wall motion. Second, a cavitary tomographic examination provides volumes of the LV, which are then analyzed by our method.

Images were acquired by a double-head DST gamma camera (SMV, Buc, France) in a tomographic mode with 32 projections of 64×64 matrix pixels (calibrated to 3 mm) over 180°. The reconstruction was performed by filtered back projection using the 'tomogated SPECT' software on a NXT console (SMV, Buc, France). Finally, 16 three-dimensional images of the heart were available within a cardiac cycle.

Due to the limited dimension of nuclear medicine images, the number of initial samples of the reconstructed

Table 1
Regional ejection fractions of the synthesized ellipsoid, with additive white Gaussian noise

| Noise | AP | LA | AA | SA | IA | LM | AM | SM | IM | LB | AB | SB | IB |
|---|---|---|---|---|---|---|---|---|---|---|---|---|---|
| 0 | 0.5 | 0.7 | 0.5 | 0.5 | 0.6 | 0.5 | 0.5 | 0.3 | 0.5 | 0.5 | 0.5 | 0.7 | 0.5 |
| 10% | 0.4918 | 0.7004 | 0.5002 | 0.5000 | 0.6000 | 0.5003 | 0.5007 | 0.2999 | 0.5000 | 0.5005 | 0.5001 | 0.7003 | 0.5000 |
| 20% | 0.4911 | 0.7009 | 0.5004 | 0.5001 | 0.6000 | 0.5005 | 0.5015 | 0.2998 | 0.5000 | 0.5009 | 0.5001 | 0.7006 | 0.5000 |

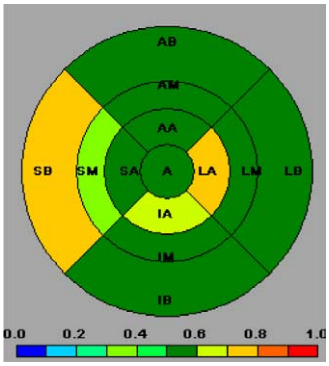


Fig. 11. Bull's-eye of local ejection fractions estimated from the synthesized ellispoid.

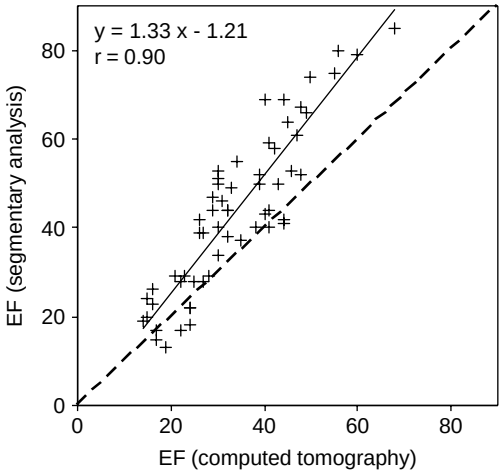


Fig. 12. Comparison of global ejection fractions measured by planar gamma-angiography and cavitary tomography (averaging, in this case, local ejection fraction values).

LV surface is small. Therefore, we chose to perform the 3DHM algorithm with a 32×32 grid, which represents a good trade-off between the number of initial samples, number of interpolated values, and computation time.[3] In the Fourier space, a rectangular filter 4×8 selects the complex coefficients that contribute to the low-pass filtering. Under these conditions, a maximum error of 1% between interpolated and initial samples of the LV surface is usually obtained in 90 iterations.

The in vivo validation consisted first in comparing the ejection fraction values obtained in planar gamma-angiography with the mean of the ejection fractions obtained in each region of interest of the LV in tomography. We checked that the results obtained are little affected by the parameters of the segmentation. Fig. 12 shows a good correlation ($r=0.90$) between the two series of measures, despite an over-estimation of about 10% of the averaged ejection fractions. This difference is most probably related

[3] About 10 s with Pentinum4 1.5 GHz computer equipped with 256 Mb RAM.

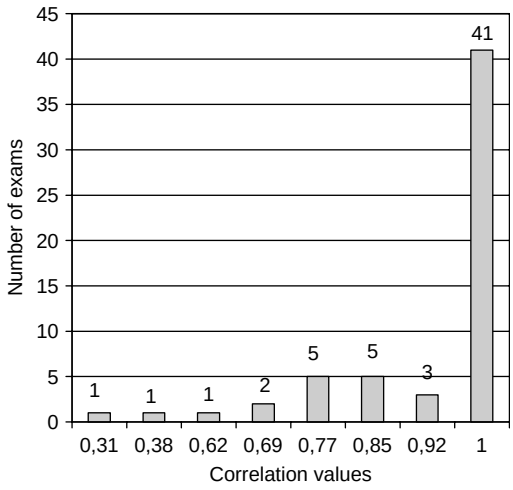


Fig. 13. Distribution of the correlation indicators of the regional contractions observed by planar gamma-angiography and cavitary tomography.

to the superposition of the left auricle during the reconstruction of volumes by tomography, which increases the ejection fraction values proportionally.

In the absence of an established gold standard for local measurements, it is difficult to validate our regional results with other techniques. We chose to compare them with results observed in planar gamma-angiography. To accomplish this, a cardiologist processed blindly planar gamma-angiography images in reference to any cavitary tomographic data. A 'score' of wall motion between 1 and 4 was assigned to each region of interest described in Fig. 5: 1 for normal wall motion, 2 for hypokinesia, 3 for akinesia, and 4 for dyskinesia. For the same patient, the corresponding regions of interest were compared for both examinations: value +1 (respectively, −1) was assigned to each pair of regions that present similar wall motion (respectively, different). By summing the values and normalizing between 0 and 1, a correlation indicator is constructed within each region. Fig. 13 shows the histogram of correlation indicators of the 59 examinations carried out. The average correlation indicator is equal to 0.92, and 70% of the measures match perfectly. The majority of the differences observed was due to the rough localization of the wall motion anomalies observed in planar gamma-angiography. Anomalies of regional wall motion were noticed for patients with ischemic cardiopathies, and agreement with planar gamma-angiography was 87%. In the population of patients with dilated cardiomyopathies, no anomaly in regional wall motion analysis was observed for 87% of the cases. For other patients, anomalies in regional wall motion analysis were identified, in concordance with planar gamma-angiography, that could correspond to sequela of myocardial infarction with healthy coronaries in two cases, and with left bundle branch block in one case.

Identification and quantification of the spread of regional anomalies is an important parameter for the management of

dilated cardiomyopathies with ischemic etiology, and for their prognostic evaluation. This parameter can be taken into account under therapeutic aspects for revascularization indication and, in a more or less near future, for cellular transplantation. The regional quantification of ejection fractions allows the comparison of results obtained from several imaging modalities with the same patient.

## 4. Conclusion and future work

This paper presents a method to analyze the local wall motion of the left ventricle of the heart. The algorithm implemented is composed of two parts. First, a kind of pre-processing uniformly re-samples initial LV surfaces using the Fourier transform, then orders the samples. No specific constraint is required on initial samples, which makes the method adaptable to many medical imaging modalities. In a second step, the algorithm divides the LV surface to create regions of equivalent volume, and local cardiac parameters are estimated: volume evolution curves as a function of time, ejection fractions, end-diastolic and end-systolic volumes and instants. The algorithm was implemented in a clinical software used routinely in a cardiology department. Results are displayed under presentations adapted to several medical specialties. After validation using surfaces generated from a deformable ellipsoid model, the method was tested on a set of patients presenting anomalies of cardiac wall motion. Local results obtained after reconstruction of LV surfaces from cavitary tomography were compared to classical 2D planar gamma-angiography examinations. Results showed a strong correlation between the two experiments, but our method provides a faster and more precise location of wall motion anomalies.

The preliminary results already obtained can be improved in two ways. Theoretically, a direct interpolation on non-uniform samplings could replace the iterative method implemented here on regular samplings using the Fourier Transform. This would involve developing a direct algorithm to interpolate surfaces with missing samples. A preliminary 1D study showed that the classical Shannon interpolation remains optimal when used with samples selected in successive intervals of equal length rather than at uniform abscissas. This study also confirmed that infinite summation of the algorithm can be replaced by finite summations, still working with non uniform samplings. After having quantified in 1D the distortions introduced by reconstruction, the results have to be extended to higher dimensions. Regarding the regional analysis, the segmentation of the global volume in regions of equivalent volume does not produce regional volumes whose surface intersection with the whole ventricle are comparable. A division in equivalent surfaces, rather than equivalent volumes, would optimize the regional analysis, because the apical regions are under-represented at present. In the same manner, a study of the local wall motion (local velocity and phase of the regional wall variation) could provide information about regional kinetic, and increase the number of indicators of the myocardic wall regional motion.

The regional analysis of the evolution of the left ventricular surfaces can also be used to compare locally different reconstructions of the ventricle. It will be exploited to validate a new technique of reconstruction of the cardiac deformations, obtained from echographic images acquired with a rotating trans-thoracic ultrasound probe during a single cardiac cycle [22].

## Acknowledgements

The authors wish to thank the French Ministry of Research (Incentive Concerted Actions) and the French National Agency of Research Valorization (ANVAR) for their financial supports, and the Segami Corporation company for its participation in this project.

## References

[1] Frangi AF, Niessen WJ, Viergever MA. Three-dimensionnal modeling for functional analysis of cardiac images: a review. IEEE Trans Med Imaging 2001;20(1):2–25.
[2] C. Vuille, A.E. Weyman, Left ventricle I: general considerations, assessment of chamber size and function. In: Weyman AE, editor. Principles and practice of echocardiography, Philadelphia; 1994.
[3] Kennedy JW, Baxley WA, Figley MM, Dodge HT, Blackmon JR. Quantitative angiocardiography: I. The normal left ventricle in man. Circulation 1966;34(1):272–8.
[4] Corbett JR, Jansen DE, Willerson JT. Radionuclide ventriculography: II. Anatomic and physiologic aspects. Am J Physiol Imaging 1987; 2(2):85–104.
[5] Hermann HJ, Bartle SH. Left ventricular volumes by angiocardiography: comparison of methods and simplification techniques. Cardiovasc Res 1968;2(4):404–14.
[6] Dodge HT, Sandler H, Baxley WA, Hawley RR. Usefulness and limitations of radiographic methods for determining left ventricular volume. Am J Cardiol 1966;18(1):10–24.
[7] Force TL, Folland ED, Aebischer N, Sharma S, Parisi AF. Echocardiography assessment of ventricular function. In: Marcus ML, Schelbert RJ, Skorton DJ, Wolf GL, editors. Cardiac imaging. London: WB Saunders; 1991. p. 374–401.
[8] Yamazaki J, Naitou K, Ishida S, Uno N, Saisho K, Munakata T, et al. Evaluation of left ventricular wall motion and function in patients with previous myocardial infarction by three-dimensional 99mTc-HSAD multigated cardiac pool imaging. Ann Nucl Med 1997;11(2): 129–38.
[9] Lessick J, Fisher Y, Beyar R, Sideman S, Marcus ML, Azhari H. Regional three-dimensional geometry of the normal human left ventricle using cine computed tomography. Ann Biomed Eng 1996; 24(5):583–94.
[10] Rademakers FE, Bogaert J. Left ventricular myocardial tagging. Int J Card Imaging 1997;3(3):233–45.
[11] Coppini G, Poli R, Valli G. Recovery of the 3-D shape of the left ventricle from echocardiographic images. IEEE Trans Med Imaging 1995;14:301–17.

[12] Nichols K, Lefkowitz D, Faber T, Folks R, Cooke D, Garcia EV, et al. Echocardiographic validation of gated SPECT ventricular function measurements. J Nucl Med 2000;41:1308–14.
[13] Nakajima K, Higuchi T, Taki J, Kawano M, Tonami N. Accuracy of ventricular volume and ejection fraction measured by gated myocardial SPECT: comparison of four software programs. J Nucl Med 2001;42:1571–8.
[14] Sharir T, Berman DS, Waechter PB, Areeda J, Kavanagh PB, Gerlach J, et al. Quantitative analysis of regional motion and thickening by gated myocardial perfusion SPECT: normal heterogeneity and criteria for abnormality. J Nucl Med 2001;42: 1639–42.
[15] Glamann DB, Lange RA, Corbett JR, Hillis LD. Utility of various radionuclide techniques for distinguishing ischemic from nonischemic dilated cardiomyopathy. Arch Intern Med 1992;152: 769–72.
[16] Iskander S, Iskandrian AE. Prognostic utility of myocardial viability assessment. Am J Cardiol 1999;83:696–702.
[17] Bardinet E, Cohen LD, Ayache N. Tracking and motion analysis of the left ventricle with deformable superquadrics. Med Image Anal 1996;1(2):129–49.
[18] Clarysse P, Friboulet D, Magnin I. Tracking geometrical descriptors on 3-D deformable surfaces: application to the left-ventricular surface of the heart. IEEE Trans Med Imaging 1997; 16(4):392–404.
[19] Jacob G, Noble AJ, Kelion AD, Banning AP. Quantitative regional analysis of myocardial wall motion. Ultrasound Med Biol 2001;27(6): 773–84.
[20] Shi P, Sinusas A, Constable RT, Ritman E, Duncan JS. Point-tracked quantitative analmysis of the LV motion from 3D images sequences. IEEE Trans Med Imaging 2000;19(1):36–50.
[21] Bonciu Cl, Weber R, Léger C. 4D reconstruction of the left ventricle during a single heart beat, from ultrasound imaging. Image Vis Comput 2001;19(6):401–4 [Elsevier Eds].
[22] Canals R, Lamarque; G, Chatain P. Volumetric ultrasound system for left ventricle motion imaging. IEEE Trans Ultrason Ferroelectr Freq Control 1999;46(6):1527–38.

**François Bernis** is an engineer specialized in computer science and interactive multidimensional applications. He graduated from the École Polytechnique of the University of Orléans. France, in 2000, and received a diploma of technological research in 2001. He is currently working as an engineer in the industry.

**Christophe Léger** received a Ph.D. degree in Sciences for Engineering from the University of Orléans, France, in 1993. Since 1994 he has been working in the same institution as an assistant professor, teaching signal and image processing and software-related courses at the Engineer school "Polytech' Orléans". He is with the Laboratory of Electronics, Signals, Images, where he leaded the LV4D (Left Ventricle of the heart in 4 Dimensions) team from 1998 to 2003. His primary research interests concern biomedical imaging. He has been working on the visualization of the volumic deformations of the left ventricle of the heart, using ultrasound images. He is currently involved in medical image registration. He has been collaborating for clinical validations and medical applications with the cardiology and nuclear medicine departments of the Hospitals of Orléans and Tours, France.

**Véronique Eder** is a Medical Doctor at the Trousseau Universitary Hospital Centre of Tours, France. She heads the "Labpart" laboratory of the University of Tours. She performs scientific research in the field of cardiovascular diseases, and focuses on the use of nuclear medicine imaging for ventricle function evaluation, especially for regional wall motion analysis of the left and right ventricles of the heart, and asynchronism assessment.